Development of CNAFT Model for Lower Flammability Limits of Hydrogen Mixtures for Severe Accident Analysis Code in Nuclear Power Plant

Jeon J.[1], Jung H.[1], Kim S.J.[1,2], *

[1] Department of Nuclear Engineering, Hanyang University, Seoul, Republic of Korea
[2] Institute of Nano Science & Technology, Hanyang University, Seoul, Republic of Korea
*Corresponding author's email: sungjkim@hanyang.ac.kr

ABSTRACT

After Fukushima-Daiichi accident, predicting lower flammability limits (LFL) of hydrogen has became an ever-important task for safety of nuclear industry. Experimental identification of LFL for all mixtures in accident conditions is considerably difficult due to wide variety of mixture types. For this reason, we have been developed a calculated non-adiabatic flame temperature (CNAFT) model to facilitate prediction of LFL. The uniqueness of this model is its ability to incorporate heat loss due to radiative heat transfer from flame during propagation using the CNAFT coefficient. The CNAFT model is more consistent with the experimental results for various mixtures compared with the previous model, which relied on the calculated adiabatic flame temperature (CAFT) to predict the LFL. However, the current model does not make a reasonable prediction of LFL under mixtures containing steam. Because steam is classified as radiating species, the presence of steam in the initial condition results more radiant heat loss. Therefore, we developed the extended CNAFT model through simulation of a seven-step combustion mechanism to consider steam effect on radiant heat loss. The extended model shows the maximum relative error with experimental results for various mixture types about 13 % even for containing steam. This study suggests that extended CNAFT model can be effectively utilized for flammability prediction in severe accident analysis code.

KEYWORDS: Hydrogen, lower flammability limit, radiative heat transfer, CAFT, CNAFT.

INTRODUCTION

After Fukushima-Daiichi accident, Korea Hydro & Nuclear Power (KHNP) classified hydrogen combustion phenomena as a major threat to containment integrity [1]. The lower flammability limit (LFL) is the minimum fuel concentration, at which a flame can propagate. If the mole fraction of the released hydrogen exceeds the LFL, a more detailed risk analysis of the NPP should be performed to verify the potential risk of flame acceleration (FA) and detonation. Because hydrogen explosions diverting to FA or detonation may add significant dynamic pressure and temperature loads that can affect containment integrity [2]. In severe accident analysis, it is of obvious importance to clarify the LFL of hydrogen mixtures under different mixture conditions. The flammability limits of various mixtures have been determined through many experimental studies [3-7]. Nevertheless, experimental identification of LFL for all mixtures during severe accident is considerably difficult due to wide variety of mixture types. Evaporation of the coolant in reactor coolant system (RCS) can cause a high concentration of steam and various gases including carbon dioxide can be released by the molten corium-concrete reaction (MCCI) in reactor cavity [8, 9]. The elevated temperature and pressure also contribute to the variety of mixture conditions. However, even the MELCOR code, which is the regulatory code of severe accident analysis developed by the US Nuclear

Regulatory Committee, adopts a rather simple logic for predicting the LFL. For example, in case of upward flame propagation, the code uses a constant LFL of 4.1 vol% regardless of the mixture conditions [10]. Such simplified LFLs can increase the uncertainty of the results on the hydrogen risk of NPPs.

Therefore, it has been considered mandatory to develop a theoretical model to reasonably predict the LFL in contingency with mixture conditions. Recently, Vidal et al. pointed out that calculated adiabatic flame temperature (CAFT) is a powerful model for estimating the LFL of gaseous mixtures [11]. The model has the advantage that it does not involve the complex algorithms considering peculiarities of the chemical kinetics of gaseous organic substances in air. It concluded that the threshold peak temperature for flame propagation was proportional to the CAFT. However, researchers have found that relying on the CAFT concept tends to result in inconsistent accuracy depending on the mixture conditions as shown Fig. 1. The mixture conditions for this model validation is shown in Table 1. This is especially true when the initial temperature of mixture is high or the diluent gas is helium or steam. The limitations of the CAFT model came from its reliance on an adiabatic value whereas actual flame propagation involves heat loss mechanisms. Many thermal theories of the flammability limits attributed the existence of the LFL to heat loss from the reaction zone [12-14]. The amount of heat loss substantially affects the peak flame temperature and hence determines the intrinsic LFL value of the mixture.
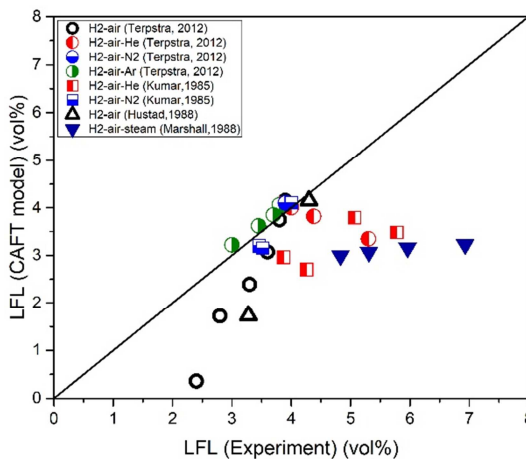

Fig. 1. Validation of CAFT model in various mixture conditions

For this reason, Jeon et al. proposed a calculated non-adiabatic flame temperature (CNAFT) model to predict the LFL considering heat loss mechanism together with the concept of the CAFT model [15]. The proposed model analysed the physics of flame propagation in a non-adiabatic condition that focused on heat loss mechanisms during upward propagation. It confirmed that radiative heat loss dominantly determines the total amount of the heat loss from the reaction zone to the ambient environment. However, the current CNAFT model does not make a reasonable prediction of LFL under mixture conditions with steam. Because steam is classified as radiating species, the presence of steam in the initial condition results more radiant heat loss. Since most mixtures during nuclear reactor accident contains steam, the current model has limitation on the hydrogen risk of NPPs.

Therefore, the objective of this study is to extend the CNAFT model to predict mixtures with steam. The amount of radiant heat loss was estimated based on the optically thin radiation model that can be used for lean hydrogen mixture conditions. Also seven-step chemical kinetics was solved for prediction of steam concentration in burned gas. As it becomes able to predict the increased amount

of heat loss by higher steam concentration, the range of model reliability was extended to H_2-Air-Steam. The validation was also carried out for mixture conditions in Table 1.

MODELLING

Concept of calculated adiabatic flame temperature

According to Arrhenius theory [16], the peak temperature occurring at the flame front determines the chemical reaction rate because the number of molecules participating in the reaction increases by the temperature. The threshold peak temperature is the temperature that can produce the minimum reaction rate to sustain propagation [17]. Previous studies concluded that the threshold peak temperature being determined by fuel type was proportional to the CAFT of the limiting mixtures. Because direct prediction of the peak temperature is almost impossible, representing the peak temperature using the CAFT was frequently done for LFL predictions in the previous studies [11]. The CAFT can be calculated from the energy balance of the reaction at equilibrium as shown in Eq. (1), where $\Delta H_{f,i}^0$ is the formation enthalpy of species i and T_{ref} is the reference temperature. The average heat capacity $\bar{c}_{p,i}^0$ was calculated for each compound using the corresponding adiabatic flame temperature,

$$\sum n_i \left[\Delta H_{f,i}^0 \right]_{reactants} - \sum n_i \left[\Delta H_{f,i}^0 + \bar{c}_{p,i}^0 \left(T_{CAFT} - T_{ref} \right) \right]_{products} = 0 \ . \tag{1}$$

However, the limitation of this concept was confirmed through experimental results in Table 1. These experiments identified the LFL near atmospheric pressure according to initial conditions such as the diluent concentration or initial temperature of the mixture. The H_2-Air-Steam flammability data was fit with the empirical equation based on results of Marshall's experiment Based on the conditions of the limiting mixtures, the value of CAFT was determined by Eq. (1). It should be noted that, although the temperature remains nearly constant for some mixtures at approximately 600 K, other mixtures show significant differences. This is especially true when the initial temperature is high or the diluent gas is steam and helium. As a result, it was confirmed that the model showed inconsistent accuracy depending on the mixture conditions as shown Fig. 1. These inconsistent with experimental results was also identified by Terpstra [7]. The reason was due to the simplified assumption of adiabatic flame expansion. In reality, however, flames do not propagate under adiabatic conditions, and heat loss processes play a part. This implies that the effects of heat loss depending on the mixture conditions cannot be ignored when predicting the LFL. In other words, the CAFT model can be applied in limited cases because it cannot account for heat transfer from the reaction zone to the environment. For this reason, Jeon et al. proposed a CNAFT model to predict the LFL considering heat loss mechanism together with the concept of the CAFT model.

Table 1. Various experimental results used in model validation

Reference	Mixture	T_i (°C)	Diluent (vol%)	CAFT (K)
Kumar [3]	H_2-O_2-He	20-100	0-40	670-800
	H_2-O_2-N_2	20-100	0-40	590-630
Hustad [4]	H_2-Air	20-200	0	610-720
Marshall [5]	H_2-Air-Steam	100-120	0-40	730-850
Terpstra [7]	H_2-Air	20-300	0	580-750
	H_2-Air-He	20	0-50	580-780
	H_2-Air-Ar	20	0-60	~580
	H_2-Air-N_2	20	0-20	~590

Non-adiabatic flame temperature model

As many theories have concluded, the effects of the heat loss from the reaction zone to the post-reaction zone play an important role in determining the peak temperature. That is to say, the heat loss mechanism ultimately affects the flammability limit of mixtures [12-14]. The essential heat loss mechanisms for laminar flame are the convective and radiative heat transfer from the flame to the environment [18]. However, convective transfer can be ignored if the tube diameter is larger than a certain value. Fernandez-Galisteo explained that it is because the burnt temperature is close to crossover value for lean flames close to the flammability limit [19]. This approach can be applied for a standard apparatus for determining the flammability limits, as done by Coward and Jones. Such apparatus consisted of a vertical tube 51 mm in diameter and 1.8 m long, closed at the upper end and open to the atmosphere at the bottom [20]. Therefore, the effect of radiative heat loss has been dominantly adopted as the explanation of the flammability limit [21].

The effects of radiative heat loss from the flame to the ambient environment can be classified as conduction of heat into the post-reaction zone, which is cooled via radiative heat loss $q_{rad,1}$ and radiative heat loss from the reaction zone itself, $q_{rad,2}$ [18]. First, the heat conduction into the post-reaction zone is caused by the temperature gradient near the end of the reaction zone. In steady-state one-dimensional flame propagation, the energy balance in the post-reaction zone can be defined as in Eq. (2), where R is the radiative volumetric heat loss and depends on the mixture properties and the local temperature distribution in the post-reaction zone, and k is the thermal conductivity. In this study, the effect of a specific flame structure depending on mixture conditions was not considered. Because the combustion regime of the observed cap-like flames at the ultralean H_2-Air mixture is not fully understood [22]. Although the approach with the one-dimensional energy equation is difficult to depict local heat transfer phenomena, it makes possible to estimate sum of heat loss in the reaction zone. Mayer noted that the diffusion term on the left is much smaller than the convection term in the region of peak flame temperature over the range of mass flow rates in typical flame propagation [18]. It means that the $q_{rad,1}$ can be calculated with peak temperature gradient under the influence of radiative heat loss as shown in Eq. (3). The equation consists of several variables determined by the mixture properties. The thermal conductivity value is based on flame front temperature, while the density and specific heat are based on the unburned gas temperature,

$$\rho_u c_p S_u \frac{dT}{dx} - \frac{d}{dx} k \frac{dT}{dx} = -R(T) \,, \tag{2}$$

$$\left(\frac{dT}{dx}\right)_{x=x_f} = -\frac{R(T_f)}{\rho_u c_p S_u(T_f)} \;\rightarrow\; q_{rad,1} = -k_f \left(\frac{dT}{dx}\right)_{x=x_f} = k_f \frac{R(T_f)}{\rho_u c_p S_u(T_f)} \,. \tag{3}$$

Second, the radiative heat loss rate from the reaction zone itself can be calculated via integration of the space-averaged radiative volumetric heat loss. However, Lakshmisha et al. proved that the fraction of $q_{rad,2}$ was very small compared to heat release rate for CH_4-Air. They numerically solved the equations for premixed flames near lean flammability limits, considering detailed chemistry and variable properties [23]. Recently, Liaw et al. confirmed that the effect of $q_{rad,2}$ is non-sizable on the H_2-Air mixtures as well as the CH_4-Air mixture by comparison between their model and experimental results [24]. These conclusion are also consistent with the experimental observations of Shoshin et al. that limit flame extinction behavior is connected with the formation of the stagnation zone of combustion products. They pointed out that the reaction zone is effectively cooled by heat conduction to the stagnation zone, which rises upward together with flame and cooled due to radiation heat loss [25]. As a result, most of the heat loss needed for calculating the peak temperature can be estimated only by considering $q_{rad,1}$.

As shown in Eq. (4), the magnitude of the radiative heat loss rate can be determined using the thermal diffusivity, flame speed, and volumetric heat loss rate. In ultralean H_2-Air flames, the laminar flame speed is severely affected by cellular instabilities as the stretch rate approaches zero. This is the profound characteristic for unstretched flames that the Lewis number is much smaller than one [26]. The flame speed of the limiting mixtures is independent of the mixture properties and its finite value can be calculated from the results presented by Davies and Taylor. Their observations were derived from experimental results, which proved that an upward propagating flame at the limit of flammability has properties in common with a rising Taylor bubble of hot gas [27]. On the other hand, according to a previously proposed optically thin radiation model, volumetric heat loss rate is determined by the threshold peak temperature and the presence of radiating species [28]. Because the threshold peak temperatures of the limiting mixtures were assumed to be invariable, the volumetric heat loss rate was considered to be constant with the exception of mixtures containing the radiating species. Consequently, the radiative heat loss rate $q_{rad,1}$ can be estimated using a linear function of thermal diffusivity through experimental and theoretical evidence. In conclusion, Jeon et al. proposed a parameter of calculated non-adiabatic flame temperature (CNAFT) through Eq. (5) to predict the LFL for each mixture condition [15]. He expected that the limiting hydrogen mixtures have similar value of CNAFT as similar with concept of CAFT. Thermal diffusivity is divided by the molar concentration C to predict heat loss in mole units. This coefficient was defined as a CNAFT coefficient, π, which can be calculated as the mean value of the physical properties of each gas component of the mixture,

$$q_{rad,1} = k_f \frac{R(T_f)}{\rho_u c_p S_u(T_f)} = \alpha \frac{R(T_f)}{S_u(T_f)} \sim \alpha , \tag{4}$$

$$\sum n_i \left[\Delta H_{f,i}^0\right]_{reactants} - \sum n_i \left[\Delta H_{f,i}^0 + \bar{c}_{p,i}^0 \left(T_{CNAFT} - T_{ref}\right)\right]_{products} = Q_{rad,1} \sim \alpha/C . \tag{5}$$

The mechanistically derived Eq. (5), which considers that radiative heat loss and the linearly proportional CNAFT coefficient, was validated using the experimental results of Terpstra and Marshall presented in Table 1. To validate this linear relationship, a reference mixture was required, and this condition was selected to be the H_2-Air mixture at 20 °C. It is because the heat loss effects on LFL is noticeable from the CNAFT coefficient on the ambient air condition. The LFL prediction in the adiabatic condition does not make noticeable error until the coefficient value at the reference mixture. Thus, the difference in heat loss was inversely estimated using Eq. (11) based on 581 K which is value of CAFT at the reference mixture. The difference in CNAFT coefficient was also calculated based on the reference mixture. The thermal conductivity used for calculating the coefficient was substituted with a corresponding value at this temperature. Figure 2 shows the difference in volumetric heat loss for each mixture based on their initial mole number before the reaction. As a result, a proportional relationship between the two variables was confirmed and Eq. (6) was determined by a least-squares analysis with R-square value of R^2-0.98. It implies that they show a strong linear relationship except for H_2-Air-Steam. Also, it should be noted that the elevated initial temperature mixtures or helium mixtures have higher CNAFT coefficient than other mixtures. Because these two types of mixtures are representative mixtures, predicting the LFL is difficult with the CAFT model, we concluded that there is a direct relationship between the overestimated CAFT and the high CNAFT coefficient of these limiting mixtures. In other words, a mixture having a high coefficient requires more combustion heat to compensate for its higher radiative heat loss than other mixtures

$$Q_{rad,1}(\pi) = 0.246(\pi - \pi_{air,20°C}), \ \pi = \alpha/C \ 10^3 \ cm^5/(mol \cdot s). \tag{6}$$
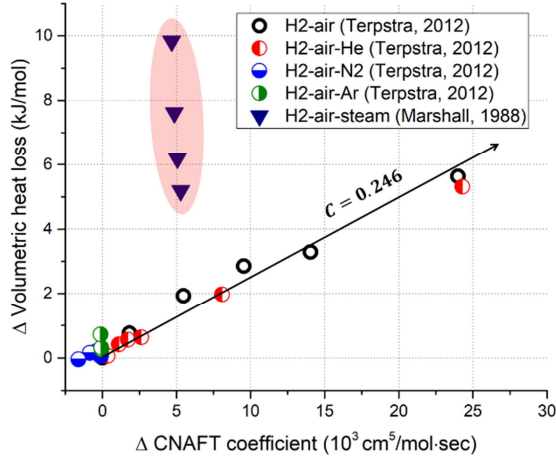
Fig. 2. Linear relationship between the CNAFT coefficient and radiative heat loss.

THE ROLE OF STEAM IN RADIANT HEAT LOSS

The reason why the linear relation between the CNAFT coefficient and radiative heat loss was not identified only for the H_2-Air-Steam mixtures can be explained by the optically thin approximation. Since the flame thickness at the flammability limits was very small, the assumption of optically thin conditions is justified by referring to the Hottel's charts. Therefore, the volumetric radiative heat loss can be calculated by Eq. (7) [20], where σ is the Stefan-Boltzmann constant, T_0 is the ambient temperature, p_{steam} is the partial pressure of steam and a_{steam} is the Planck's mean absorption coefficient of steam. The independence of the peak flame temperature and mixture conditions remains as before. It should be noted that, in the case of a mixture containing steam, the volumetric rate increases proportionally as the partial pressure of steam increases. In other words, the volumetric rate cannot be assumed to be constant as in a mixture without steam. Therefore, the total amount of radiative heat loss during flame propagation of a mixture with steam under isobaric condition can be estimated by Eq. (8). The reference value $X_{steam,ref}$ is the steam mole fraction at the flame front during flame propagation in mixtures without steam. Even if there is no steam in the initial mixture, steam can be produced through the combustion process. However, it was deduced that the variation of the steam concentration was negligible in other diluent types through confirmation of the proportional relationship between the CNAFT coefficient and the amount of heat loss. It is because the difference of initial hydrogen concentration between the limiting mixtures is sufficiently small. Therefore, the amount of heat loss in a mixture containing steam can be estimated if the value of steam mole fraction at the flame front during propagation $X_{steam,flame\ front}$ can be predicted,

$$R = 4\sigma\left(T_f^4 - T_0^4\right) p_{steam} a_{steam} , \tag{7}$$

$$Q_{rad,1}(\pi) = 0.246\left(\pi - \pi_{air,20°C}\right)\left(X_{steam,flame\ front} / X_{steam,ref}\right). \tag{8}$$

Fernandez-Gasliteo showed, for hydrogen-air mixtures that are very fuel lean, the seven-step mechanism including three reversible shuffle reactions 1-3 and the irreversible recombination 4f suffices to describe accurately progress of combustion as shown Table 2. Therefore, in this study, the mechanism was solved to predict the variation of the steam mole fraction during combustion process [29]. Because the rate coefficient in the Arrhenius form $k = AT^n \exp(-T_a/T)$ constants for all reactions, the reaction rate is calculated solely as a function of temperature. The backward rate of reactions 1-3 are approximate fits calculated from the forward parameter using the thermodynamic

data. In calculating the pressure dependence of the reaction rate constant, the value of falloff factor F_c was determined by the previous computation by Troe [30].

Table 2. The 7-step mechanism with rate coefficient in the Arrhenius form [24]

Reactio□		A	n	$T_a[K]$
1. $H + O_2 \leftrightarrow OH + O$		3.52□+16	-0.7	8590
2. $H_2 + O \leftrightarrow OH + H$		5.06□+04	2.67	3166
3. $H_2 + OH \leftrightarrow H_2O + H$		1.17□+09	1.3	1829
4f. $H + O_2 + M \rightarrow HO_2 + M$ ∗	k_0	5.75□+19	-1.4	0
	k_∞	4.65□+12	0.44	0
5f. $HO_2 + H \rightarrow OH + OH$		7.08□+13	0	148
6f. $HO_2 + H \rightarrow H_2 + O_2$		1.66□+13	0	414
7f. $HO_2 + OH \rightarrow HO_2 + O_2$		2.89□+13	0	-250

In the case of combustion of limiting mixture with very low flame speed, the structure at the flame front can be predicted by computation of homogenous ignition above crossover temperature. Figure 3 shows the verification of our computation by a typical time history obtained ignition above crossover temperature for a stoichiometric H_2-Air mixture with San Diego mechanism obtained from Ref. [19]. It was identified that the seven-step chemistry provides a sufficiently accurate results in the temporal evolution of hydrogen mole fraction. Although the temperature change shows a slight difference, it is clear that this difference will be further reduced in lean conditions. It means that the steam mole fraction at flame front during propagation of hydrogen lean flame can be predicted by this simplified chemistry.
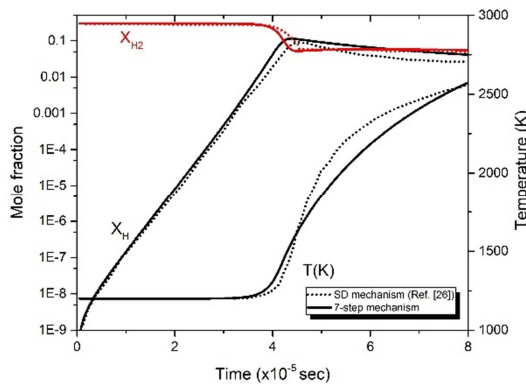

Fig. 3. Code validation for ignition of stochiometric H_2-Air mixture in a homogenous adiabatic reactor at constant atmospheric pressure and initial temperature $T = 1200$ K.

Figure 4 shows the temporal evolution of hydrogen and steam mole fraction for each limiting mixture during homogenous ignition above crossover temperature. When the steam concentration is zero, the LFL is 3.9% and it burns completely in a very short time. This aspect is equally founded in the other three cases with steam, and the steam mole fraction in burned gas is very close to the sum of initial hydrogen and steam mole fraction. This complete combustion in the hydrogen lean condition with steam was identified not only in this homogeneous ignition simulation, but also in a

computation of steady planar deflagration obtained with COSILAB code [19]. However, as mentioned, the specific modes of flame propagation were observed such as cap-like flames in ultraliean H2-Air flames. These observed natures can affect the steam concentration near the end of the reaction zone. This is our further study.
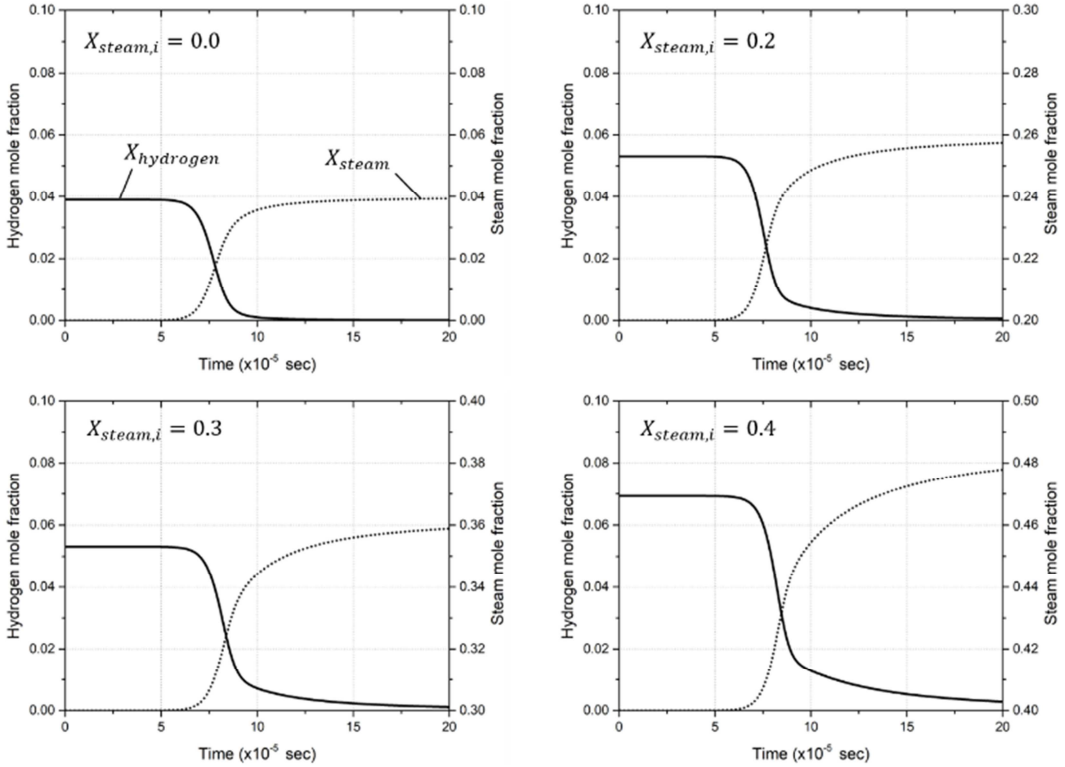

Fig. 4. Temporal evolution of $X_{hydrogen}, X_{steam}$ for each limiting H2-Air-Steam mixture as obtained from numerical integrations with 7-step mechanism of Table 1 ($X_{steam} = 0.0, 0.2, 0.3, 0.4$).
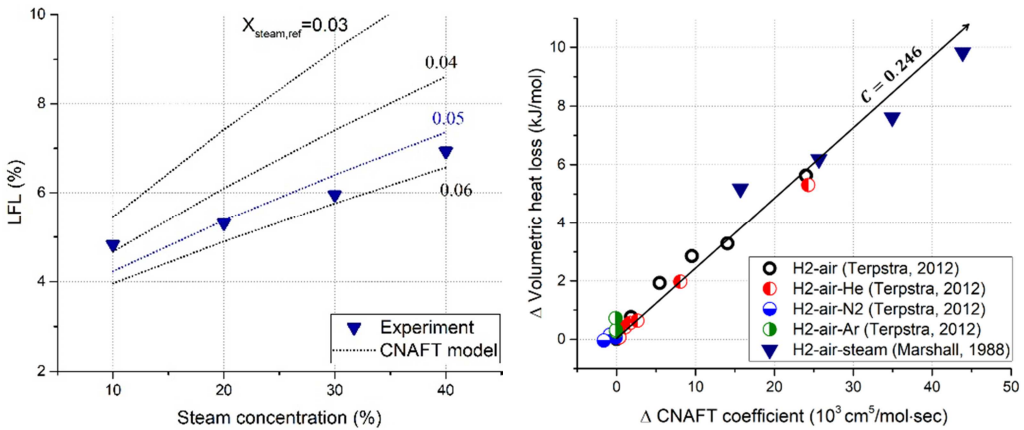

Fig. 5. Sensitivity analysis for determination of optimum reference steam mole fraction (left) and linear relationship between the extended CNAFT coefficient and radiative heat loss with $X_{steam,ref} = 0.05$ (right).

In conclusion, the calculation of steam concentration during flame propagation under each limiting mixture condition can be substituted by a complete combustion approach as shown Eq. (9). The amount which can be estimated by the initial condition including CNAFT coefficient and initial mole fraction increases proportionally as the sum of initial hydrogen and steam mole fraction increases. The reference steam mole fraction, which was neglected to predict the heat loss of mixtures without steam, was determined by sensitivity analysis. Because the mixtures without steam produce steam at flame front as hydrogen combustion proceeds, the reference mole fraction will be in the LFL range of 0.03-0.06. Therefore, the sensitivity analysis was performed to obtain the optimum value for estimation of radiant heat loss based on the range as shown Fig. 5. It was confirmed that the average prediction accuracy was the highest when the reference mole fraction was set to 0.05. Although this approach for averaged reference temperature may cause non-negligible errors, this empirical derivation was considered to essential for predicting the LFL in a H_2-Air-Steam mixture. The term of steam effect can be negligible when no steam is present in the initial mixture,

$$Q_{rad,1}(\pi) = 0.246(\pi - \pi_{air,20°C})(X_{H_2,initial} + X_{steam,initial})/X_{steam,ref} .$$ (9)

RESULTS AND DISCUSSION

The accuracy of the CNAFT model and extended CNAFT model was compared in Fig. 6 based on the experimental results in Table 1. For mixtures without steam, both models show reasonable accuracy because the radiant heat loss increases due to helium concentration or high temperature can be predicted by the CNAFT coefficient. However, in the case of the mixture containing steam, the current CNAFT model has a consistent tendency to predict higher LFL values than the experimental values. This is because the amount of radiant heat loss, which increases with the presence of steam in the initial condition, was underestimated. On the other hand, the extended CNAFT model shows high accuracy for all listing mixtures as consideration of steam effect on radiant heat loss except for a H_2-Air-He mixture. The reason was a significantly large thermal diffusivity value of the mixture compared to other mixtures because of both high temperature and helium concentration ($X_{He} = 40\%, T_i = 100 °C$). The maximum relative error was 13 % except for the mixture. As as result, by knowing the initial condition of a mixture for which the LFL is not known experimentally, the amount of heat loss in the CNAFT model can be estimated. Then, the hydrogen concentration at which the CNAFT reaches 581 K according to Eq. (5) and (9) is the LFL value predicted by the CNAFT model.
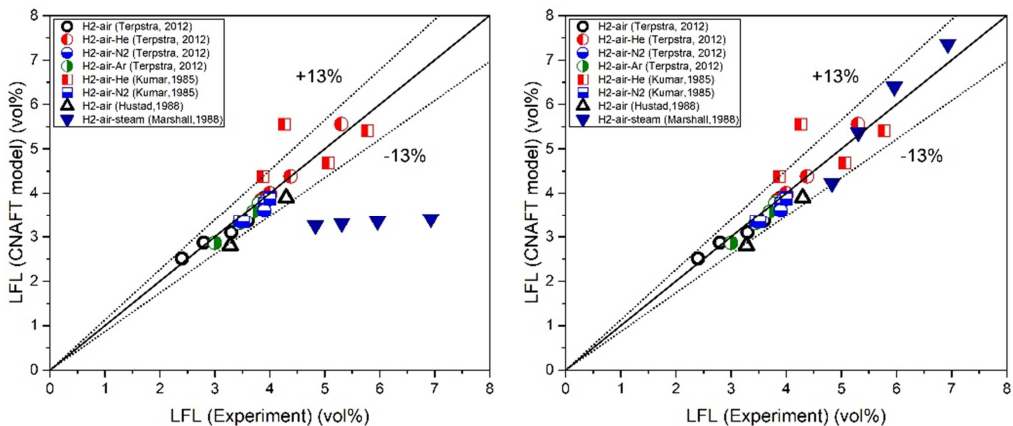

Fig. 6. Validation of CNAFT model in various mixture conditions (left: current, right: extended).

CONCLUSIONS

In this study, the extended CNAFT model was developed to predict the LFL of H_2-Air-Steam mixture based on the heat transfer mechanisms during flame propagation. The simulation of seven-step combustion mechanism provided a rationality for a complete combustion approach in terms of predicting the steam mole fraction at the flame front. Agreement with experimental LFL results on H_2-Air-Steam mixtures was improved significantly, for which the current CNAFT model showed technical limitations. We confirmed that considering radiative heat loss induced by steam mole fraction is essential for estimating the peak flame temperature for various mixture conditions. This study suggests that extended CNAFT model can be effectively utilized for flammability prediction in severe accident analysis code. Our major findings and future work can be summarized as follows.

- The reason why the current CNAFT coefficient cannot proportionally estimate the amount of radiant heat loss for H_2-Air-Steam mixtures can be explained by the optically thin approximation. In the case of a mixture containing steam, the radiant volumetric rate increases proportionally as the partial pressure of steam increases.

- The seven-step simulation for combustion process of liming H_2-Air-Steam mixtures identified that the steam mole fraction in flame front is very close to the sum of initial hydrogen and steam mole fraction regardless of the initial steam mole fraction.

- The amount of heat loss in a mixture containing steam can be estimated with the complete combustion approach. The amount which can be estimated by the initial condition including CNAFT coefficient and initial mole fraction increases proportionally as the sum of initial hydrogen and steam mole fraction increases.

- However, the specific modes of flame propagation were observed such as cap-like flames in ultraliean H2-Air flames. These observed natures can affect the steam concentration near the end of the reaction zone. This is our further study.

ACKNOWLEDGEMENT

REFERENCES

[1] M.R. Seo, Status of Severe Accident Analysis for New Accident Management Plan, Trans. Korean. Nucl. Soci., Jeju, Korea, 2017.

[2] N.K. Kim, J. Jeon, W. Choi, S.J. Kim, Systematic Hydrogen Risk Analysis of OPR1000 Containment before RPV Failure Under Station Blackout Scenario, Ann. Nucl. Energy 116 (2018) 429–438.

[3] R. K. Kumar, Flammability Limits of Hydrogen-Oxygen-Diluent Mixtures, J. Fire Sci. 3 (1985) 245-262.

[4] J.E. Hustad, O.K. Sønju, Experimental Studies of Lower Flammability Limits of Gases and Mixtures of Gases at Elevated Temperatures, Combust. Flame 71 (1988) 283-294.

[5] B.W. Marshall, Hydrogen:Air:Steam Flammability Limits and Combustion Characteristics in the FITS Vessel, Report No. SAND84-0383, Sandia National Lab., 1986.

[6] Y.N. Shebeko, S.G. Tsarichenko, A.YA. Korolchenko et al., Burning Velocities and Flammability Limits of Gaseous Mixtures at Elevated Temperatures and Pressures, Combust. Flame 102 (1995) 427-437.

[7] M. Terpstra, Flammability Limits of Hydrogen-Diluent Mixtures in Air, MSc thesis, University of Calgary, Canada, 2012.

[8] W. Choi, S.O. Yu, S.J. Kim, Efficacy Analysis of Hydrogen Mitigation Measures of CANDU Containment under LOCA Scenario, Ann. Nucl. Energy 118 (2018) 122-130.

[9] T. Kim, W. Choi, J. Jeon, N.K. Kim, H. Jung, S.J. Kim, A Conceptual Approach to Eliminate Bypass Release of Fission Products by In-Containment Relief Valve under SGTR Accident, Sci. Technol. Nucl. Install. Vol. 2018, Article ID 5936214, 12 p.

[10] R.O. Gauntt et al., MELCOR Computer Code Manuals Version 1.8.6, Report No. SAND2001-0929P, Sandia National Lab., 2005.

[11] M. Vidal, W. Wong, W.J. Rogers, M.S. Mannan, Evaluation of Lower Flammability Limits of Fuel–Air–Diluent Mixtures using Calculated Adiabatic Flame Temperatures, J. Hazard. Mater. 130 (2006) 21–27.

[12] H.Y. Shih, Computed Extinction Limits and Flame Structures of H2/O2 Counterflow Diffusion Flames with CO_2 Dilution, Int. J. Hydrogen Energy 34 (2009) 4005-4013.

[13] J.S. Ha, C.W. Moon, J. Park et al., A Study on Flame Interaction between Methane/Air and Nitrogen-Diluted Hydrogen-Air Premixed Flames, Int. J. Hydrogen Energy 35 (2010) 6992-7001.

[14] P.G. Holborn, P. Battersby et al., Modelling the Effect of Water Fog on the Upper Flammability Limit of Hydrogen-Oxygen-Nitrogen Mixtures, Int. J. Hydrogen Energy 38 (2013) 6896-6903.

[15] J. Jeon, N. K. Kim, W. Choi, T. Kim, S. J. Kim, Investigation of Flammability of Hydrogen Gases with Diluent Gases under Severe Accident Conditions using CNFT Model, Int. Con. Nucl. Eng., London, England, 2018.

[16] I. Glassman, R.A. Yetter, N.G. Glumac, Combustion, Academic press, 2014.

[17] D.M. Himmelblau, J.B. Riggs, Basic Principles and Calculations in Chemical Engineering, FT press, 2012.

[18] E. Mayer, A theory of Flame Propagation Limits due to Heat Loss, Combust. Flame 1 (1957) 438–452.

[19] D. Fernandez-Galisteo, A.L. Sanchez, A. Linan, F.A. Williams, The Hydrogen-Air Burning Rate Near the Lean Flammability Limit, Combust. Theor. Model. 13 (2009) 741-761.

[20] H.F. Coward, G.W. Jones, Limits of Flammability of Gases and Vapors, US Bureau of Mines, Bulletin 627, Pittsburgh, Pennsylvania, USA, 1952.

[21] C.K. Law, F.N. Egolfopoulos, A Unified Chain-Thermal Theory of Fundamental Flammability Limits, Proc. Combust. Inst. 24 (1992) 137–144.

[22] Z. Zhou, Y. Shoshin, F.E. Hernandez-Perez, et al., Experimental and numerical study of cap-like lean limit flames in H_2-CH_4-air mixtures, Combust. Flame 189 (2018) 212-224.

[23] K.P. Lakshmisha, P. Paul, H. Mukunda, On the Flammability Limit and Heat Loss in Flames with Detailed Chemistry, Proc. Combust. Inst. 23 (1991) 433–440.

[24] H.J. Liaw, K.Y. Chen, A model for predicting temperature effect on flammability limits, Fuel 178 (2016) 179-187.

[25] Y. Shoshin, J. Jarosinski, On extinction mechanism of lean limit methane-air flame in a standatd flammability tube, Proc. Combust. Inst. 32 (2009) 1043–1050.

[26] Y. Dong, A.T. Holley, M.G. Andac, et al., Extinction of premixed H_2/air flames: chemical kinetics and molecular diffusion effect, Combust. Flame 142 (2005) 374-387.

[27] A. Levy, An Optical Study of Flammability Limits, Proc. R. Soc. Lond. A. 283 (1965) 134–145.

[28] Y. Ju, G. Masuya, P.D. Ronney, Effects of Radiative Emission and Absorption on the Propagation and Extinction of Premixed Gas Flames, Proc. Combust. Inst. 27 (1998) 2619–2626.

[29] D. Fernandez-Galisteo, A.L. Sanchez, A. Linan, F.A. Williams, One-Step Reduced Kinetics for Lean Hydrogen-Air Deflagration, Combust. Flame 156 (2009) 985-996.

[30] J. Troe, Detailed Modeling of the Temperature and Pressure Dependence of the Reaction H+ O2 (+ M)→ HO2 (+ M), Proc. Combust. Inst. 28 (2000) 1463–1469.